applied sciences

Article

Research on Interference Mechanism of 25 Hz Phase Sensitive Track Equipment from Unbalanced Current

Lei Wang [1], Benchao Zhu [1], Jingcao Chen [2], Mingchao Zhou [1], Zhengyan Liu [1], Jinyan Li [1] and Chunmei Xu [1,*]

[1] School of Electrical Engineering, Beijing Jiaotong University, Beijing 100044, China; leiwang@bjtu.edu.cn (L.W.); 18126190@bjtu.edu.cn (B.Z.); 19121544@bjtu.edu.cn (M.Z.); 17291122@bjtu.edu.cn (Z.L.); 21121439@bjtu.edu.cn (J.L.)
[2] China Railway Shanghai Group Co., Ltd., Shanghai 201800, China; 22121466@bjtu.edu.cn
* Correspondence: chmxu@bjtu.edu.cn

Abstract: In a 25-Hz phase-sensitive track circuit, traction backflow is unevenly distributed in the two rails, resulting in interference caused by the 50 Hz unbalanced current, which leads to misoperation of relays and other equipment in the circuit. Focusing on the mechanism of unbalanced current generation, this paper probes the causes of track circuit equipment interference and innovatively analyzes the mechanism of the choke transformer and relay affected, in order to find a method to suppress the interference of the 25 Hz phase-sensitive track equipment. Firstly, the mechanism of unbalanced current generation is explained, and the influence of the unbalanced impulse current on the choke transformer and binary two-bit relay is analyzed. Secondly, the DC magnetic bias, the second side voltage of the choke transformer and the excitation current, flux density, core loss of choke transformer and relay under a different unbalance impulse current are simulated. Then, the unbalanced current simulation test, unbalanced current test during driving and grounding wire test are carried out. Finally, it is concluded that the unbalanced impulse current causes magnetic saturation of the choke transformer, then affects voltage sag of the relay coil, resulting in misoperation of equipment. The conclusions of this paper can play an important guiding role in studying the influence of unbalanced current and restraining the interference of the 25 Hz phase-sensitive track circuit.

Keywords: 25 Hz Phase-Sensitive track circuit; red ribbon; track reflux; traction power supply; unbalanced current

Citation: Wang, L.; Zhu, B.; Chen, J.; Zhou, M.; Liu, Z.; Li, J.; Xu, C. Research on Interference Mechanism of 25 Hz Phase Sensitive Track Equipment from Unbalanced Current. *Appl. Sci.* **2023**, *13*, 1033. https://doi.org/10.3390/app13021033

Academic Editors: Xingxing Jiang and Xiaojian Yi

Received: 19 December 2022
Revised: 7 January 2023
Accepted: 9 January 2023
Published: 12 January 2023

1. Introduction

With the development of electrified railways, scholars in many countries have gradually attached importance to research on track circuit disturbance caused by the traction return system. At present, the railway traction return system adopted in France includes rails, chokes, grounding wires, grounding electrodes, protection wires and equipotential bonding wires between conductors. However, the channel of the signal circuit is not the rail, and the through ground wire is used as the return wire in parallel with the rail [1]. The railway traction return system adopted in Germany consists of rail, return line, catenary, equipotential bonding line between conductors, grounding terminal, etc. [2].

The rail circuit is a circuit composed of rail as the transmission medium, electrically isolated at both ends, and connected with the power transmission and receiving equipment [3]. At present, nearly 98% of stations on electrified railways use 25 Hz phase-sensitive track circuits [4]. The unbalanced current generated by unbalanced factors such as track imbalance and adjacent rail interference in the track circuit will invade the equipment. When the rail unbalanced current is too large, it will cause interference to the equipment, which is likely to cause the circuit to flash red and other misoperations, leading to emergency braking of the train, affecting traffic safety [5]. Therefore, it is necessary to study the unbalanced current in the 25 Hz phase-sensitive track circuit. The research is of great significance to the analysis of equipment malfunction in the track circuit.

Aiming at the problem of the unbalanced current of the track circuit, Hu Xiaosheng pointed out from the view of signal maintenance that the causes of the unbalanced traction current of two rails mainly include the reasons of the signal equipment itself, the improper position of the tower ground wire on the rail on one side of the track circuit and suction line [6]. Yet, he did not analyze the internal mechanism of the unbalanced current and the interference mechanism of the choke transformer, relay and other equipment from a theoretical point of view. Ming Jianhao explained the traction return current distribution model in three ways: direct power supply, current absorption transformer power supply and autotransformer power supply. He introduced the causes of the unbalanced current but did not consider the unbalanced current caused by hanging the grounding wire, and did not analyze the impact of unbalanced current in detail [7]. Yao Linlin and Jin Laisheng pointed out that the unbalanced impedance of the rail will lead to the generation of unbalanced current, and it will interfere with the choke transformer and signal equipment [8,9]. However, they did not explain the interference caused by adjacent tracks of the 25 Hz track circuit and did not consider the effect on the coils of the operating device. Based on the theory of rail transit line impedance and admittance, Hill et al. obtained the self impedance and mutual impedance of the track under power frequency, but they did not further study the influence of impedance on the traction return current [10]. Hossein Arghavani et al. pointed out that the impedance of the two rails cannot be completely equal in actual engineering. Unbalanced traction return will occur between the rails. The unbalanced current of the rails will cause the impedance of the choke transformer to increase, where the signal flow path is the rail. The unbalanced current in the rail will cause interference to the track circuit, and even damage the signaling equipment [11].

In view of the influence of the unbalanced current on track circuit equipment such as the choke transformer and binary two-bit relay, Jiang Tao, combined with the red ribbon fault, pointed out that the process of adding the ground wire to power outage equipment will change the traction return current and affect the rail current distribution and track circuit [12]. However, he only explained the source of the unbalanced current and did not analyze the specific process of interference on the equipment. J.S. Huh analyzed the influence of the unbalanced traction return current and the anti-interference direction of the track circuit [13]. Zhang Youpeng et al. analyzed the characteristics of the signal current in the adjustment state and the broken rail state of the broken rail detection circuit. Based on the analysis of the distribution and characteristics of the traction return current under the AT power supply mode, the mechanism of the unbalanced traction return current interfering with the broken rail detection circuit was deeply analyzed [14]. Yet, they did not analyze the mechanism of the influence on the key components inside the choke transformer and relay. Therefore, this paper studies the problems which are not discussed by the other scholars above, and it analyzes the action process and influence of the unbalanced current of the specific type of track circuit on equipment. The conclusion of this paper can play an important role in the research of restraining the interference of the track circuit.

Because of the above problems, this paper studies the mechanism of 25 Hz phase-sensitive track circuit equipment misoperation based on an unbalanced current. Section 2 studies the causes of the red ribbon problem, analyzes the mechanism and causes of the unbalanced current caused by the traction unbalanced current and the grounding wire, and discusses the interference of the unbalanced impulse current intrusion on the choke transformer coil and the binary two-bit relay wing plate and coil. In Section 3, the excitation current, secondary voltage, magnetic flux density, core loss of choke transformer, magnetic flux density and core loss of relay under different unbalanced impulse currents are simulated and the causes of misoperation are analyzed. In Section 4, through the unbalanced current simulation test, the unbalanced current test in the driving process, the ground wire test, combined with the test results, this paper analyzes and verifies the causes of the abnormal red ribbon phenomenon induced by the unbalanced current affecting the relay misoperation. It is concluded that under the interference of unbalanced current, the choke transformer will have magnetic saturation, which will affect the relay coil voltage and cause misoperation.

2. Cause Analysis of Abnormal Red Ribbon

Affected by the traction unbalanced current and the ground wire in the whole traction system, the receiving end track circuit will have problems such as “flashing red” due to interference. Therefore, it is necessary to clarify the mechanism of the unbalanced current generated by the above two and analyze the model when the unbalanced current invades the track circuit.

2.1. Generation Mechanism of Unbalanced Traction Current

Double choke double rail phase sensitive track circuit is generally used in the AC electrified section to realize the coding of the track and turnout section of the station, and the traction current and signal current are circulated on the rail [15]. The magnitude and direction of the traction current flowing through the rails on both sides are the same in the ideal state, but due to the existence of imbalance on both sides of the rail, there will be a difference between the two rail traction currents, that is, an unbalanced traction current [16].

2.1.1. Impedance Unbalance of Traction Current Circuit

From the traction current wheel–rail circuit shown in Figure 1, it can be seen that, after the traction current flows through the electric locomotive transformer, it finally flows into the track through the contact between the wheel and rail. The unbalance phenomenon caused by unequal impedance in the current loop is the essence of unbalanced traction current.

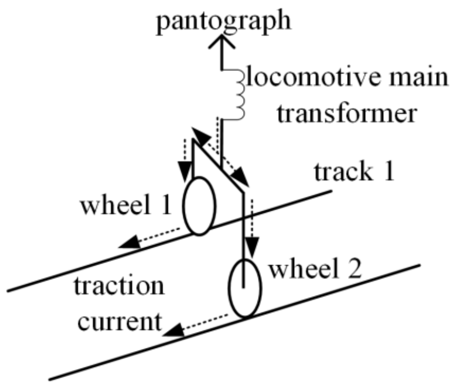

Figure 1. Traction current wheel rail circuit.

The differences in site environment and track conditions will cause inconsistent rail contact impedance. At the same time, the contact area and pressure between wheel–rail and rail are constantly changing during vehicle driving, which affects the contact impedance between wheel–rail and rail. Therefore, the unbalanced wheel–rail contact impedance and rail impedance in the current loop are the main causes of the unbalanced traction current.

2.1.2. Adjacent Rail Traction Current Interference

In order to reduce the interference caused by the adjacent track as much as possible, the rail spacing is generally recommended to be greater than 4400 mm. However, in the actual situation, the electromagnetic effect caused by the larger traction current will inevitably affect the weak electrical signal of the adjacent circuit. The schematic diagram is shown in Figure 2.

In Figure 2, the traction current of the right rail is I_1 and I_2. Electromagnetic induction will induce an induced current of I_0 in the left rail circuit, which will interfere with the left rail circuit [17]. The direction of the induced magnetic field is outward, and the size is represented by the sparsity of the dots.

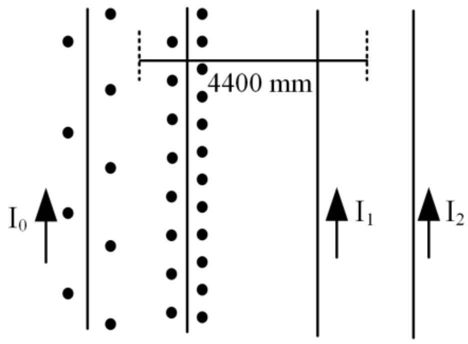

Figure 2. Magnetic field coupling in adjacent orbit.

It is assumed that the traction current of the two tracks on the right is in an ideal state, i.e., $I = I_1 = I_2$. The synthetic magnetic induction intensity can be expressed by Equation (1) [5,18].

$$B = B_1 + B_2 = \frac{\mu I}{2\pi}(\frac{1}{a} + \frac{1}{b}) = \frac{\mu I}{2\pi d} \tag{1}$$

In Equation (1), μ is the surrounding permeability; B is the synthetic magnetic field strength; the magnetic induction intensity generated by the two rails is B_1, B_2, direction from inside to outside; a and b, respectively, represent the distance between the disturbed track and the two tracks on the right; d is the equivalent distance between the equivalent current and the disturbed track $d = ab/(a + b)$.

The magnetic flux in the closed loop area of the left rail ϕ can be expressed as Equation (2).

$$\phi = \int_S d\varphi = \int_d^{d+c} \frac{\mu I}{2\pi x} l dx = \frac{\mu l I_m}{2\pi} \ln(\frac{d+c}{d}) \sin(\omega t) \tag{2}$$

In Equation (2), l is the length of the disturbed rail; I_m is the current amplitude; d represents the distance between the equivalent wire and the closed loop; c is the rail spacing; ω is the angular frequency of the current.

Correspondingly, the induced electromotive force can be expressed as Equation (3).

$$E = -\frac{d\phi}{dt} = -\frac{\mu I_m \omega}{2\pi}(\ln\frac{d+c}{d}) \cos(\omega t) \tag{3}$$

From the analysis of Equation (3), it can be seen that when the traction current is transmitted in the rail, the induced current will be generated in the adjacent return circuit due to the induced magnetic field, which will invade the adjacent track and cause an unbalanced current, thus causing interference to the adjacent track circuit. The induced current is affected by track impedance, traction current, equivalent disturbance distance, rail spacing and surrounding permeability.

2.2. Disturbance Mechanism Caused by Grounding Wire

During the daily maintenance work on the track circuit site, in order to ensure the safety of the maintenance personnel, it is necessary to construct an absolute non-electric zone with the earth as the zero point, so the grounding wire should be installed on the relevant equipment. However, in the process of track circuit section maintenance, the grounding wire is often accompanied by induction discharge. The large current generated on the track causes the unbalanced current to invade the track, then interferes with the signal in the track circuit.

The essence of the disturbance of the track circuit caused by the grounding wire is to change the impedance of one side of the track, resulting in the impedance imbalance of the two rails. When the catenary is overhauled, it is necessary to hang the grounding wire on the catenary to the single-sided grounding track, which is equivalent to the catenary in parallel to the single-sided grounding track. This will reduce the equivalent impedance of the rail of the single-sided grounding track, and the potential difference between the two rails will cause the voltage of the rail to fluctuate, causing interference to the track receiving the end equipment and causing misoperation. At the same time, part of the traction current in the non-working section will flow into the working section through the rail, resulting in an increase in the reflow imbalance between the two rails, increasing the degree of interference with the track circuit equipment.

2.3. Influence of Unbalance Current Intrusion on Choke Transformer

As shown in Figure 3, there is an insulation joint in the rail of the 25 Hz track circuit. In order to ensure the normal flow of traction current at the rail and the matching of signal transmission, we need to install a choke transformer and connect its adjacent neutral points.

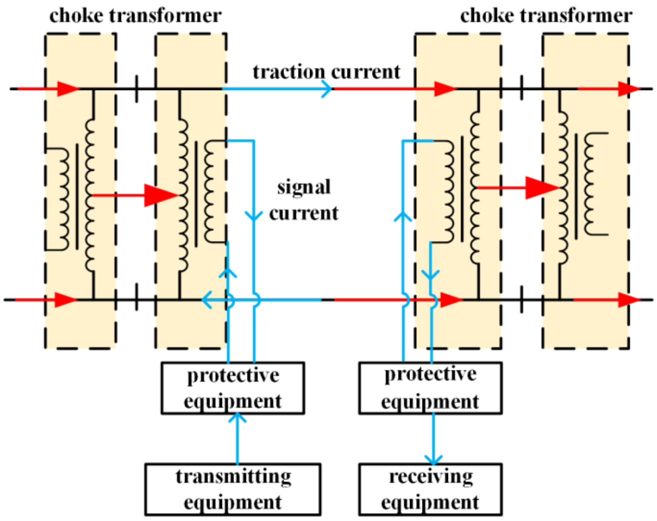

Figure 3. Signal current and traction current.

However, due to the invasion of the unbalanced current, the magnetic flux induced by the two-rail traction current flowing through the primary side of the choke transformer no longer offsets each other. The interference current generated on the secondary side invades the signal side, which affects the voltage on the signal side and causes misoperation. The following analyzes unbalanced current intrusion into the receiving end circuit choke transformer.

2.3.1. Analysis of Unbalanced Impulse Current

Unbalanced current includes steady-state unbalanced current and unbalanced impulse current. Due to the great influence of DC bias caused by unbalanced impulse current, the unbalanced impulse current is analyzed.

When unbalanced current invades the receiving end circuit, the choke transformer is the first equipment to be affected. The transient process of choke transformer can be equivalent to the transition from no-load state to load state, which will produce impulse current. Its equivalent circuit can be represented by RL zero state response, as shown in Figure 4 [19].

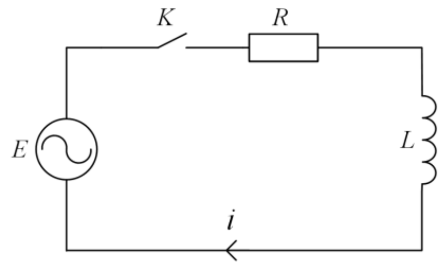

Figure 4. Equivalent circuit of unbalanced impulse current invading choke transformer.

The switching K closure is equivalent to the intrusion process of the unbalanced impulse current, which will cause the transition current i to be generated in the equivalent circuit. The transition current consists of a forced component (AC component) i_Q and a free component (DC component) i_Z, so the current can be expressed as Equation (4):

$$i = i_Q + i_Z = \frac{E \cdot \sin(100\pi t + \theta - \beta)}{\sqrt{R^2 + (100\pi L)^2}} + Ae^{-\frac{R}{L}t} \tag{4}$$

where R is the sum of copper loss and external resistance, L is the excitation inductance, E is the 50 Hz power supply, whose instantaneous expression is $E\sin(100\pi t + \theta)$, θ is the initial phase angle, $\beta = tg^{-1}(100\pi L/R)$.

Using the initial state current as zero, that is, $i_{(0)} = 0$, the value of parameter A can be solved, which is expressed as Equation (5).

$$A = -\frac{E \cdot \sin(\theta - \beta)}{\sqrt{R^2 + (100\pi L)^2}} \tag{5}$$

Let $I_M = E/\sqrt{R^2 + (100\pi L)^2}$; the final total current Equation (6) is obtained.

$$i = I_M\left[\sin(100\pi t + \theta - \beta) - \sin(\theta - \beta) \cdot e^{-\frac{R}{L}t}\right] \tag{6}$$

According to Equation (6), when $|\theta - \beta| = n\pi + \pi/2$ (n is a positive integer), the amplitude of the free component i_Z is the largest, and the amplitude is I_M. Therefore, when the inductance in the equivalent circuit is linear, the peak value of the transition current i is twice the forced component. At this time, the transformer core will be seriously saturated, which will further reduce the excitation inductance, resulting in an increase in the current in the transformer, and the saturation degree of the core will continue to increase, which will continue to affect the excitation inductance, forming a “vicious circle”. This process will eventually seriously increase the core loss of the transformer and ultimately, affect the signal circuit.

2.3.2. DC Magnetic Bias Analysis of Transformer

As the transformer is an electromagnetic device, the iron core has saturation characteristics [20]. When there is an interference current flowing into the transformer, the magnetic flux will increase on the basis of the original normal operation, and the working point will also move, making the iron core saturated; the waveform will also be distorted; and finally, the secondary side voltage will also be interfered with and reduced [21]. Through the analysis of unbalanced impulse current, it can be seen that there is a DC component in the unbalanced impulse current, which will lead to the generation of magnetic flux with the DC component in the transformer. It can be intuitively seen from Figure 5 that due to the existence of the DC component in the unbalanced impulse current, the magnetic flux curve of the transformer moves upward, which eventually causes the excitation current of the transformer to be distorted, causing interference to the track circuit equipment.

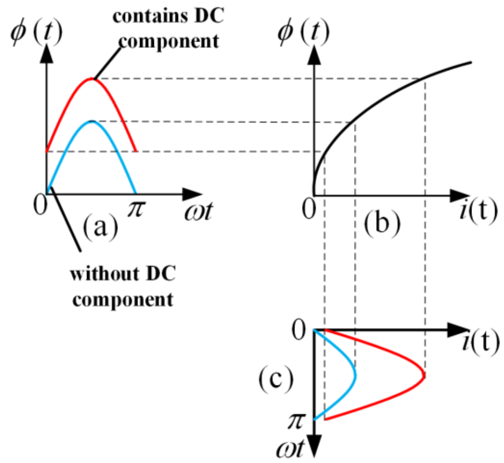

Figure 5. DC bias of choke transformer. (**a**) The change of magnetic flux curve when the impulse current flows into the transformer; (**b**) The working characteristic curve of the transformer under normal working condition; (**c**) The change of excitation waveform when the impulse current flows into the transformer.

2.4. Influence of Unbalanced Current Intrusion on Relay

2.4.1. Interference Analysis of Unbalanced Impulse Current on Relay Wing Plate

In order to simplify the research on the problem of misoperation caused by the unbalanced impulse current to relay interference, the linear inductance in the transformer is regarded as a fixed value.

For a 25 Hz track circuit, the interference frequency is 50 Hz in its two working cycles. The torque generated on the relay wing plate when the unbalanced impulse current invades can be obtained, as shown in Equation (7):

$$M = \frac{KI_G I_J}{0.08}\int_0^{0.08}\left[2\omega\sin(2\omega t+\theta-\beta+\pi/2)+p\sin(\theta-\beta)e^{-pt}\right]\cdot\sin(\omega t)dt \tag{7}$$

where the angular velocity is set to 2ω; the angular velocity of the local coil side current is set to ω; I_G is the peak current flowing through the relay track coil side; I_J is the peak current flowing through the local coil side; the time constant p is R/L; K is the structural coefficient of the binary two-bit relay.

When $\theta - \beta = \pi/2$, the relay wing plate torque is Equation (8):

$$M = \frac{KI_G I_J}{0.08}\int_0^{0.08}\left[-2\omega\sin(2\omega t)+pe^{-pt}\right]\cdot\sin(\omega t)dt \tag{8}$$

The excitation impedance angle of the transformer is set to 75°. The frequency of the unbalanced traction current is the power frequency. The time constant is the value obtained by Equation (9).

$$p = R/L = 100\pi/tg75^\circ \approx 84 \tag{9}$$

Therefore, it can be calculated that $M \approx 2.7766KI_G I_J$.

The current frequency of the coil side of the relay is 25 Hz, and the peak current is I_G. It is assumed that the relay is in the optimal pull-in state, that is, the phase lag of the track current is 90°, and the excitation inductance of the transformer is considered to be linear inductance. According to the peak value of the AC component, the torque value in two working cycles can be calculated as Equation (10).

$$M = \frac{50\pi K I_G I_J}{0.08}\int_0^{0.08} \sin^2(50\pi t)dt \approx 78.5 K I_G I_J \tag{10}$$

In practice, the maximum impulse current of the circuit is 6~8 times of the steady-state value, so the torque generated by the track coil side of the relay is about (16.7~22.2) KI_GI_J. The current parameter of the track coil side of the binary two-bit relay in the 25 Hz track circuit is 0.038 A. Therefore, when the impulse current invading the track coil side reaches 0.14 A, the torque will be disturbed, thus causing the relay to misoperate.

When $\theta - \beta = 3\pi/2$, the initial value of the DC component was $I_M \sin(\theta - \beta) = -I_M$. Therefore, the actual value of the torque generated on the relay wing when the unbalanced impulse current invades is $\pm 2.7755 K I_G I_J$. It can be seen that the interference of the unbalanced impulse current to the relay is uncertain, which may cause the relay wing to misoperate.

2.4.2. Interference Analysis of Unbalanced Impulse Current on Relay Coil

The track relay belongs to the secondary side load of the choke transformer. The interference of the impulse current will cause the magnetic saturation of the choke transformer. In order to analyze the influence of the secondary side of the transformer on the track circuit, it is necessary to simplify the choke transformer circuit.

The choke transformer model studied in this paper is BE-600/25. The number of turns of the traction coil of this type of transformer is 8 turns, a total of two groups. The signal coil has 48 turns, so the circuit diagram of the choke transformer and its equivalent circuit are shown in Figure 6.

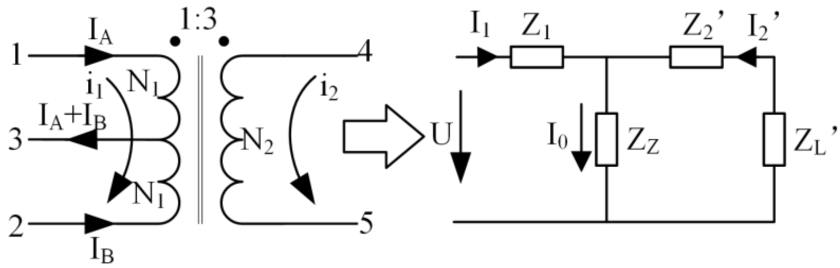

Figure 6. Choke transformer circuit and equivalent circuit.

Among them, Z_1 represents the traction side coil impedance. Z_Z represents the nonlinear excitation impedance. $Z_2{}'$ is the secondary winding impedance converted to the primary side. I_0 is the current in the nonlinear excitation impedance. I_1 is the traction coil side current. $I_{2'}$ is the signal coil side current converted to the primary side. $Z_L{}'$ is the load. Therefore, the voltage at both ends of the load $\dot{U}_L'$ can be expressed as Equation (11).

In this paper, the allowable current of the choke transformer is set to 1000 A. The primary side resistance R_1 and the secondary side coil resistance R_2 are both 0.2 Ω. The mutual inductance parameter is 11.09 mH. The secondary side load parameter R_L of the choke transformer is 6Ω. $|Z_Z|$ = 2.3 Ω, which can be ignored due to the small coil inductance. Equation (12) is thus obtained.

$$\dot{U}_L{}' = \frac{\dot{U} Z_L{}'}{(Z_1 + Z_2{}' + Z_L{}') + \frac{Z_1 Z_2{}' + Z_1 Z_L{}'}{Z_Z}} \tag{11}$$

$$\dot{U}_L{}' = \frac{0.67\dot{U}}{0.892 + \frac{0.138}{|Z_Z|}} \tag{12}$$

The circuit inside the protection box includes capacitance and inductance, which can block the 50 Hz interference source. However, due to the existence of the DC component in the impulse current, the filtering effect on the impulse current is not obvious. When the value of $|Z_Z|$ decreases from 2.3 Ω to 0.2 Ω, the load voltage $\dot{U}_L'$ decreases from 0.71 $\dot{U}$ to 0.42 $\dot{U}$. For the circuit with a choke edge, the voltage of the relay decreases by 41%. In the actual normal case, the relay pulls in when it is greater than 15 V, and falls when it is less than 8.6 V. The voltage change is 43.3%. Through the above analysis, it can be seen that when the excitation impedance continues to decrease and the core is more saturated, the relay contact will fall and a red ribbon will appear.

3. Disturbance Analysis and Simulation of Receiving Equipment

3.1. Disturbance of Unbalanced Current on Choke Transformer

3.1.1. DC Magnetic Bias of Choke Transformer

In order to clarify the interference from the DC magnetic bias of the choke transformer under an unbalanced current, the primary side of the choke transformer is connected to the 25 Hz power supply as the working power supply. The DC source is injected as the interference source. The excitation current state is analyzed when the interference source is 0 V, 0.5 V, 1 V, and 1.5 V, respectively [1,2,22].

It can be found from Figure 7 that when the DC interference source is 0 V, the excitation current is a normal sine wave. When the interference source increases to 0.5 V, the excitation current waveform begins to be affected, and the sine wave is distorted. When the interference source continues to increase, it can be clearly observed that the degree of excitation current distortion becomes more obvious. When the DC interference source reaches the maximum, the excitation current peak is greater than 5 A, the waveform peak burr is very serious, and the degree of asymmetry is also maximum.

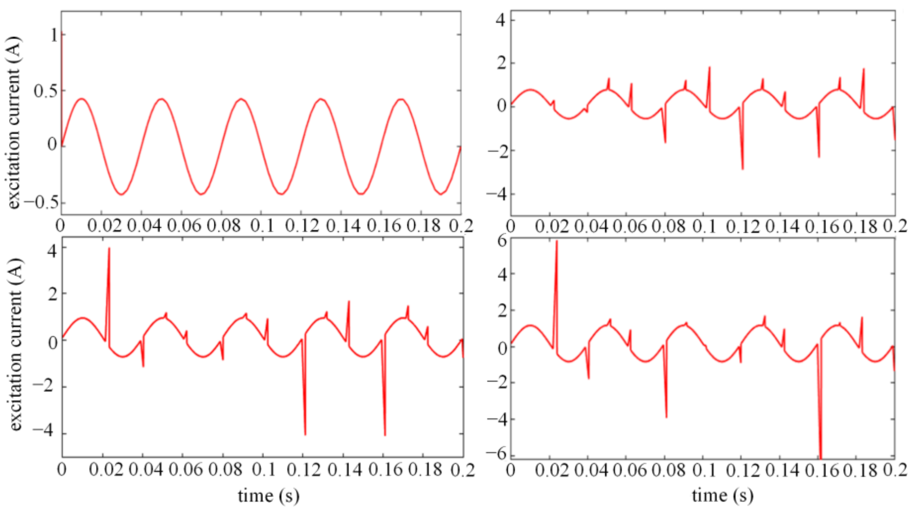

Figure 7. Waveform of excitation current under different DC interference sources.

3.1.2. Influence of Unbalanced Impulse Current on Choke Transformer

In order to study the influence of the unbalanced impulse current on the choke transformer, this paper selects the model BE-600/25 choke transformer, and simulates it under the condition of unbalanced impulse current. The parameters of the choke transformer are shown in Table 1.

Table 1. Choke transformer parameters.

	Winding Number	Winding Turns	Winging Diameter	Number of Parallel Branches	Winding Material
traction coil	2	8	10.4 × 30 mm	1	flat steel
signal coil	1	48	10.4 × 30 mm	1	electrolytic copper

In order to simulate the situation that the choke transformer is interfered, 25 Hz signal current and 50 Hz unbalanced current are added to the traction coil, in which the effective value of the signal current is 0.3 A and the frequency is 25 Hz. At the same time, the steady-state component can be set to a certain value to simulate the unbalanced impulse current, and its frequency is set to 50 Hz. The working current in the signal coil is set to 0.8 A and the frequency is 25 Hz.

The influence of DC magnetic bias on the track circuit is studied by setting different values of DC components. Therefore, the DC current values of 0 A, 0.5 A, 1.0 A, 1.5 A, 2.0 A and 2.5 A are added to the traction coil side, respectively.

The excitation current generated in the choke transformer under different DC components is shown in Figure 8. It can be observed that with the increase of the DC component in the impulse current, the excitation current in the choke transformer will also increase significantly. When the DC component value reaches 2.5 A, the DC component can cause a large enough excitation current, so that the transformer core is magnetically saturated, resulting in a decrease in the secondary voltage and affecting the working state of the track circuit.

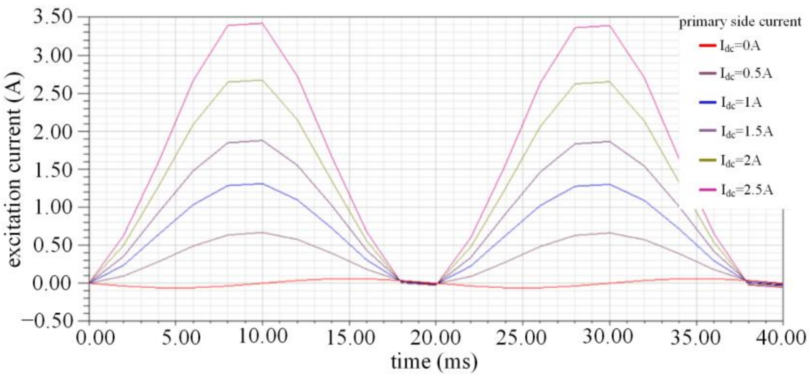

Figure 8. Excitation current of choke transformer under different DC components.

Figure 9 shows the magnetic flux density nephogram under different DC components. It can be seen that, with the increase of the DC component, the magnetic density of the choke transformer core also increases, which accelerates the process of magnetic saturation.

While the excitation current of the transformer is affected, the core loss of the transformer will also be affected by the unbalanced impulse current. Figure 10 shows the waveforms of the core loss of the choke transformer under different DC components. It can be seen that the DC component is positively correlated with the core loss of the choke transformer. When the DC component reaches the maximum value of 2.5 A, the core loss is 92 W. At this time, the core loss is serious, which makes the core temperature rise, then affects the operation state of the transformer. If it is in long-term operation, the service life of the choke transformer will be reduced due to the increase of temperature stress.

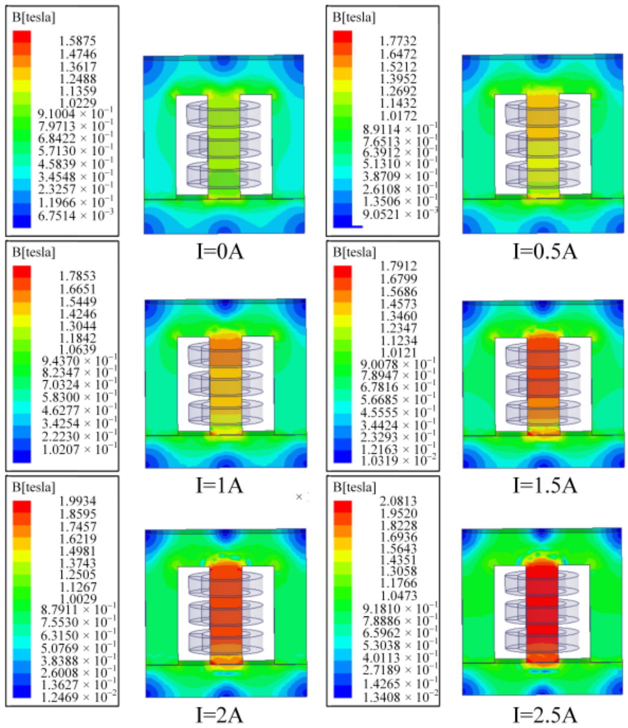

Figure 9. Magnetic flux density nephogram under different DC components.

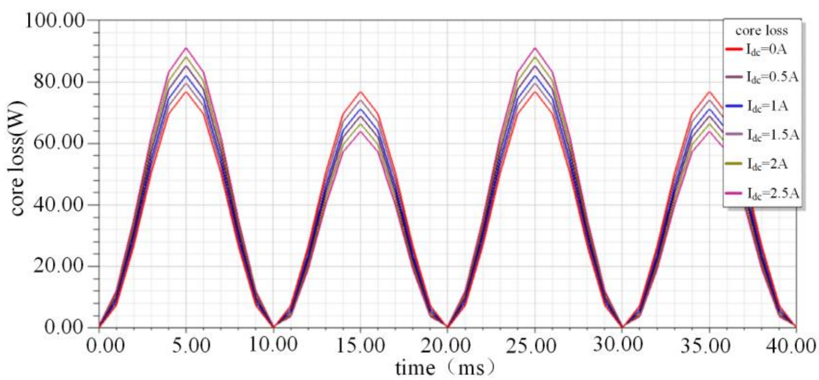

Figure 10. Loss of choke transformer core under different DC components.

For the influence of unbalanced impulse current on the secondary side of the choke transformer, it can be found from Figure 11 that the secondary side voltage of the choke transformer decreases with the increase of the DC component, and the two are negatively correlated. This is due to the increase of the excitation current, the choke transformer produces DC magnetic bias, so that the core accelerated magnetic saturation, resulting in a secondary side voltage drop. For a binary two-bit relay, the voltage drop of the track coil will cause the wing plate to fall, resulting in misoperation.

3.2. Disturbance of Unbalanced Current on Relay

Although there is a protective box on the track coil side of the relay, which can block most of the interference current, it is difficult to eliminate the interference of unbalanced impulse current due to the DC component.

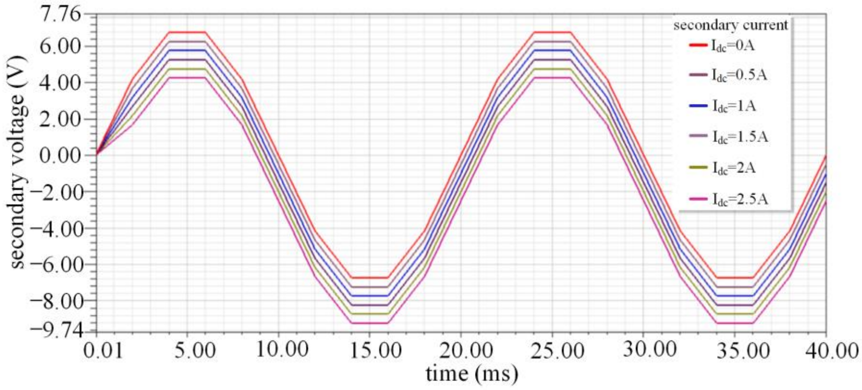

Figure 11. Secondary voltage waveform under different DC components.

The JRJC-70/240 binary two-bit relay model and its external circuit simulation model are built. The magnetic flux density and core loss of the relay coil are simulated to verify the influence of unbalanced impulse current on the relay. In order to fit the actual situation, the LC circuit analog protection box is added to the track coil side, and a 50 Hz and exponential decay power supply is introduced into the external circuit to simulate the interference source.

The relay local coil side voltage is 110 V, and the frequency is 25 Hz. The working voltage of the track coil side is 15 V, the frequency is 25 Hz, and the phase angle difference with the local coil side power supply is set to 90. In addition, the protective box is set, and the inductance is 0.845 H. The capacitance parameter is 12 µF. The added interference source waveform is shown in Figure 12.

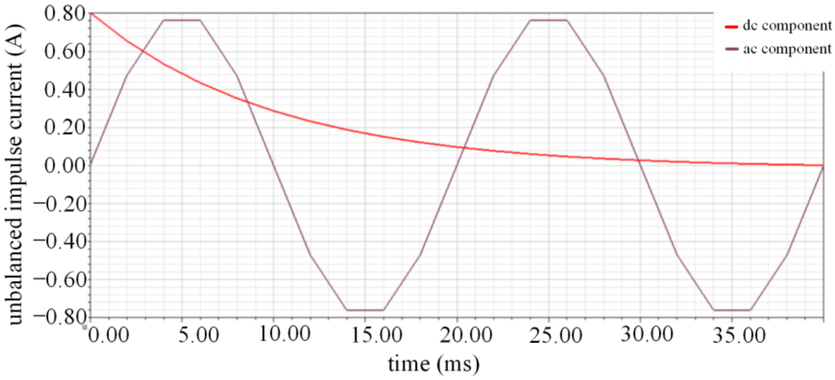

Figure 12. Impulse current interference source waveform.

By setting five unbalanced impulse current interference sources of 0 A, 0.2 A, 0.4 A, 0.6 A, 0.8 A and 1 A, the magnetic flux density and core loss of the relay are simulated, as shown in Figures 13 and 14. When the unbalanced impulse current is 0 A, the magnetic flux density and core loss are small. As the invasion current of the relay increases, the magnetic flux density and core loss also increase. When the unbalanced impulse current reaches 1 A, the core loss changes more obviously with the increase of current. This will increase the heating degree of the relay and cause the vibration of the wing plate, which may eventually lead to the appearance of an abnormal red ribbon.

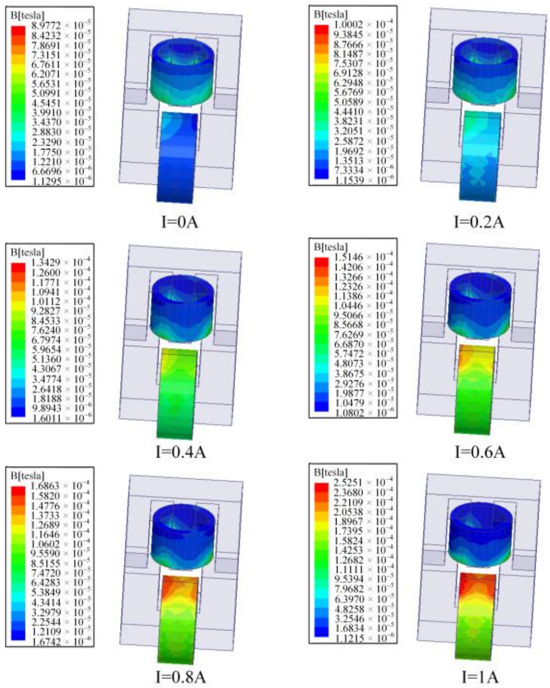

Figure 13. Relay coil flux density.

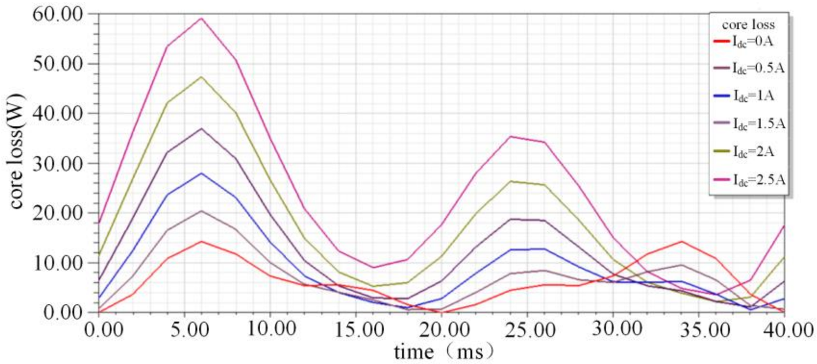

Figure 14. Relay core loss.

4. Analysis of Track Circuit Misoperation Test

In this paper, the unbalanced current simulation test, the field rail section actual measurement test and the grounding wire test are carried out under actual operating conditions to verify the analysis results of the unbalanced current affecting the track circuit leading to the misoperation.

4.1. Analysis of Unbalanced Current Simulation Test

This paper simulates the unbalanced current of one sending and one receiving section for the test. In order to simulate the state of the flash red ribbon in the field, it is necessary to inject 50 Hz unbalanced component into the 25 Hz operating waveform at the receiving end.

In this experiment, a 50 Hz voltage source is used as the excitation source of the unbalanced current. The circuit schematic is shown in Figure 15; the secondary side of the isolation transformer is connected in series with the 2 terminals of the receiving-end choke transformer, and the primary side of the isolation transformer is connected to the voltage regulator to adjust the 50 Hz unbalanced current in the 25 Hz track circuit. In order to analyze the collected waveform reliably, it is necessary to slowly increase the output voltage of the voltage regulator. In this process, collect and observe the change of 50 Hz unbalanced current of the receiving circuit until the binary two-bit relay or track relay acts, then stop increasing the voltage. Record the unbalanced current value, voltage, current and other electrical quantities of the track circuit. Voltage probes are arranged at terminals 1 and 3, 2 and 3, 4 and 5 of the choke transformer, respectively, and current probes are arranged at terminals 1 and 4. The current probe is arranged at the local coil and track coil side of the binary two-bit relay.

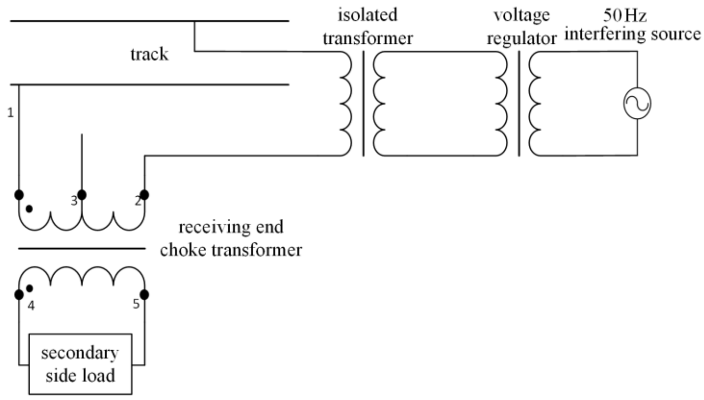

Figure 15. Unbalanced current simulation test circuit.

When the unbalanced current is not connected, the operating state waveform of the choke transformer is shown in Figure 16. It can be seen that the voltage and current frequencies of the primary and secondary sides are 25 Hz, without 50 Hz voltage and current interference. However, due to the influence of track imbalance and other factors in practice, the effective value of terminal 1 of the primary side current of the track transformer is 2.9 A, the effective value of terminal 3 of the primary side current of the choke transformer is 12.5 A, and the effective value of the secondary side terminal current of the choke transformer is 98 mA. Therefore, the unbalanced current is also generated in the track circuit, and the value is 9 A.

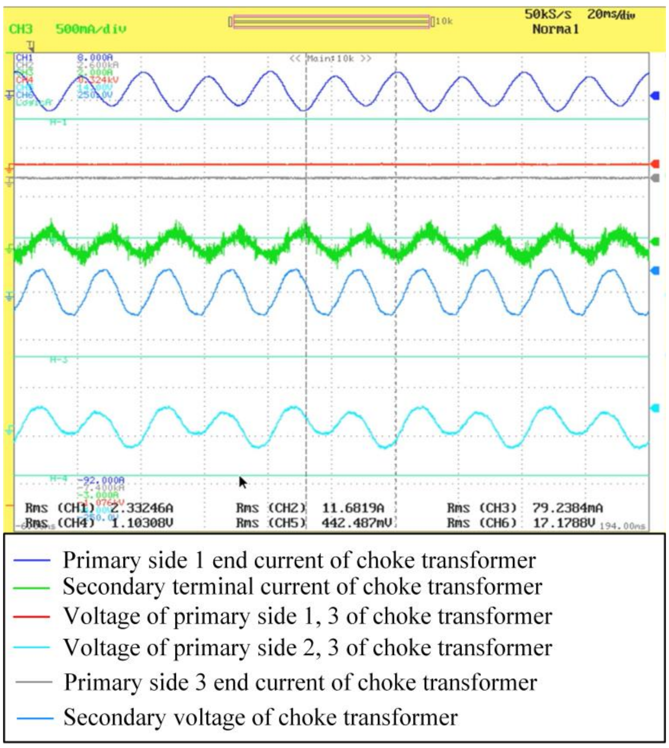

Figure 16. Choke transformer waveform without interference.

Figure 17a,b show the waveforms of the receiving end choke transformer during the simulation of the interference and the misoperation. It can be observed that the voltage and current of the primary and secondary sides of the choke transformer are disturbed by the unbalanced current. With the injection of 50 Hz interference voltage and current into the 25 Hz normal operating waveform, it can be found that the 25 Hz secondary terminal current waveform of the choke transformer is distorted. The effective values of the current on both sides of the track are 11 A and 27 A, respectively. It can be calculated that the unbalanced current in the track circuit reaches 16 A, and the choke transformer gradually enters a saturation state. It can be seen from Figure 17b that the current on both sides is 11 A and 37 A, respectively, and the unbalanced current value reaches 26 A. The choke transformer is already in a severe saturation state.

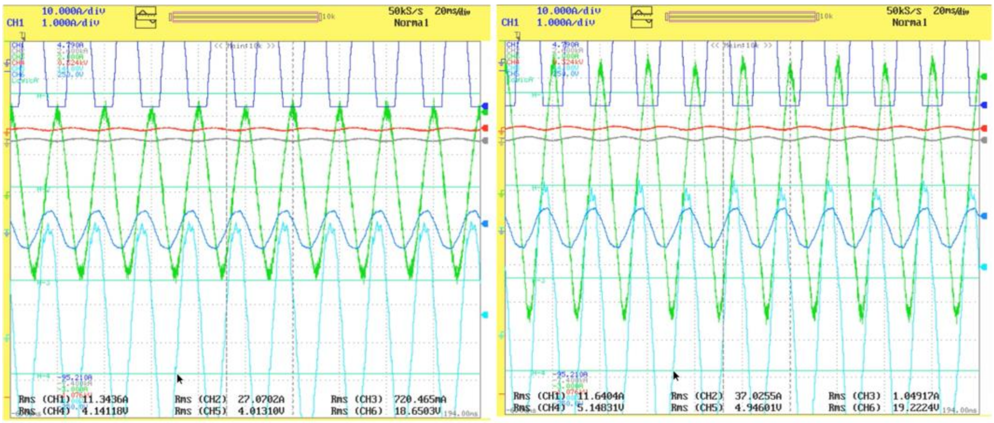

(a) (b)

Figure 17. Receiver choke transformer waveform in case of interference and misoperation. (**a**) Receiver choke transformer waveform in case of interference; (**b**) Receiver choke transformer waveform in case of misoperation.

Figure 18a,b shows the waveforms of the relay during the interference and the misoperation. It can be found that the terminal voltage of the track coil changes significantly, and some waveforms of the indoor relay are also affected when the interference source is injected. As shown in Figure 18a, the effective value of the track coil side voltage of the binary two-bit relay decreases from 22 V to 15 V. According to the release value of JRJC1-70/240 not being less than 8.6 V, the reliable drop value is 7.74 V; it can be seen that the relay operation standard is not reached at this time, and no red ribbon appears. However, by observing the relay track coil voltage in Figure 18b, it can be found that the track coil side voltage drops to 2.675 V and the distortion is serious, indicating that the relay is severely disturbed by the unbalanced current, causing the red ribbon in the track circuit, causing the track circuit misoperation. This shows that with the increase of the unbalanced current, the voltage of the relay track coil side decreases. Therefore, when the unbalanced current increases to a certain extent, the track coil side voltage drops to the relay operation value, which will cause the track circuit misoperation.

4.2. Unbalanced Current Test during Driving

Based on the simulation test of the interference source applied to the track circuit, the track circuit with voltage fluctuation is monitored. The field test wiring diagram is shown in Figure 19.

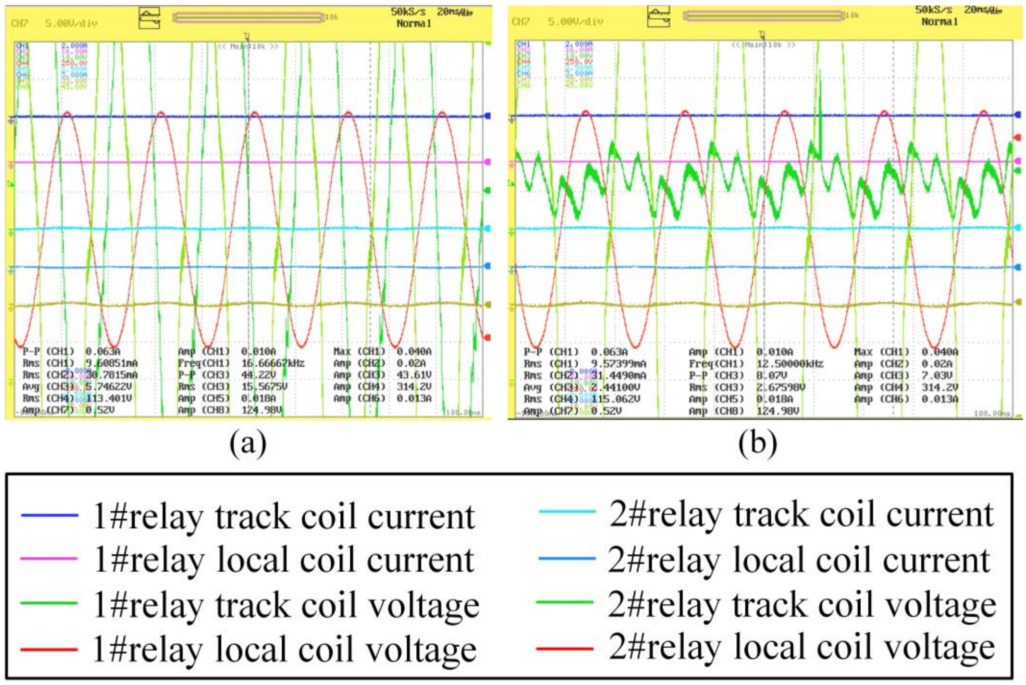

Figure 18. Receiver relay waveform in case of interference and misoperation. (**a**) Receiver relay waveform in case of interference; (**b**) Receiver relay waveform in case of misoperation.

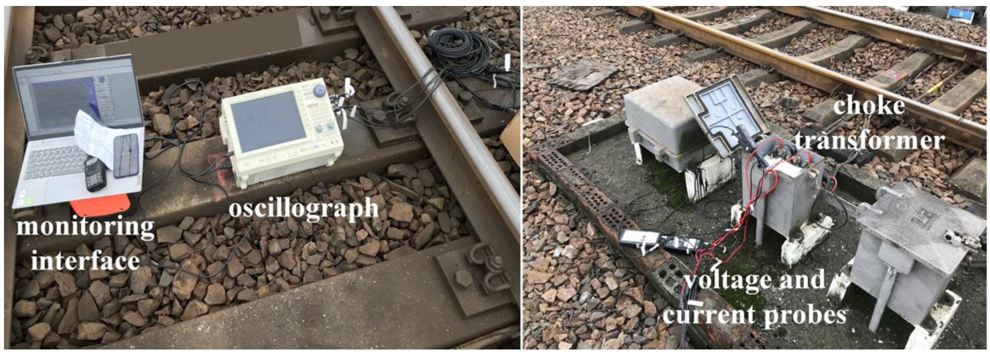

Figure 19. Layout of field measurement equipment.

Figure 20 records the waveforms of electrical quantities at the monitoring points on the monitoring road sections and other adjacent track sections during driving. In Figure 20a,b, the unbalanced current with small value is generated in the track circuit. It can be seen that the 25 Hz signal current contains a 50 Hz interference current. Figure 20c,d are the unbalanced impulse current generated in the track circuit. The current has a short time and a large amplitude, which makes the choke transformer magnetic saturation and makes the secondary side equipment disturbed. In Figure 20e,f, it can be seen that when there is traffic in other sections, the unbalanced impulse current will also bring interference to the monitored area, indicating that the unbalanced effect brought by other track traffic will affect the track, which may cause the relay track coil voltage to decrease, resulting in track circuit misoperation.

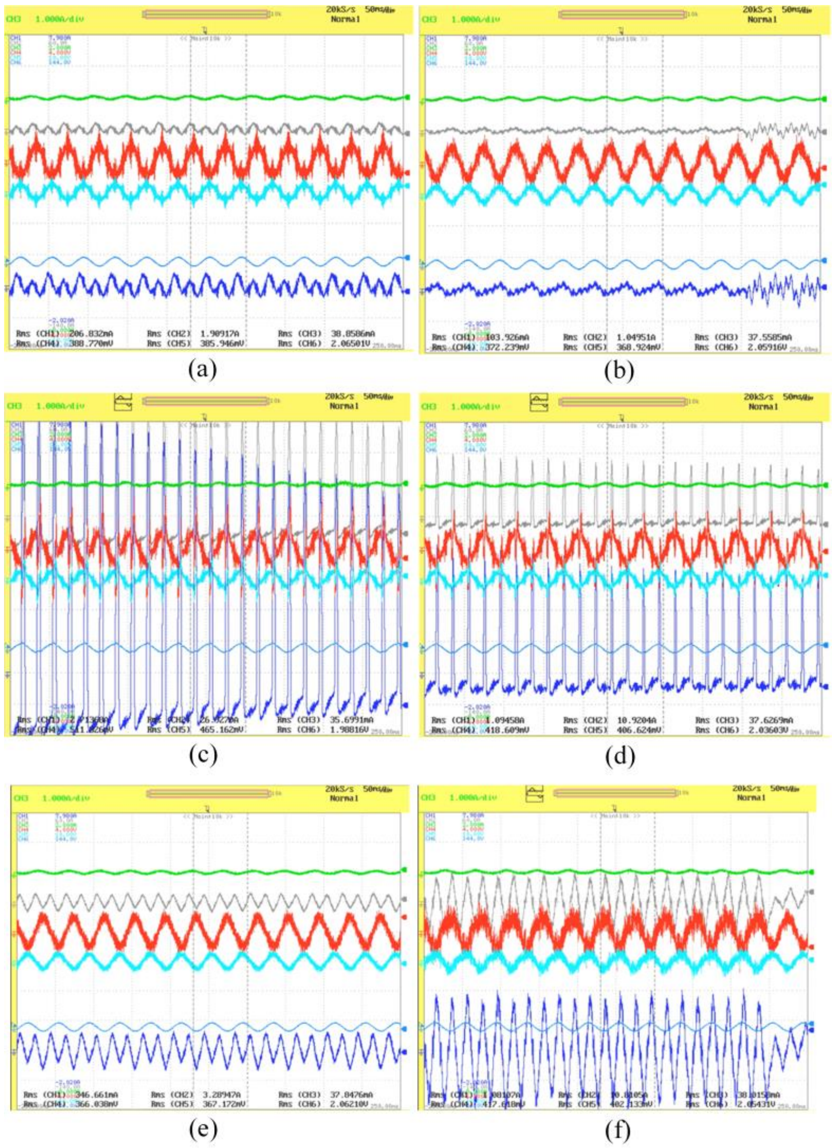

Figure 20. Unbalanced current in track circuits under different conditions. (**a**) Monitoring road section waveform when small unbalanced current is generated in track circuit; (**b**) Adjacent track section waveform when small unbalanced current is generated in track circuit; (**c**) Monitoring road section waveform when transient impulse unbalance current exists; (**d**) Adjacent track section waveform when transient impulse unbalance current exists; (**e**) Monitoring road section waveform when steady-state unbalanced current exists; (**f**) Adjacent track section waveform when steady-state unbalanced current exists.

4.3. Analysis of Hanging Ground Wire Test

After clarifying the mechanism of the red ribbon phenomenon caused by the unbalanced current generated by hanging the ground wire, the ground wire test was carried out on the site. Considering the influence of the ground wire on the adjacent track and the degree of interference, the track signal circuit of one sending and one receiving track is selected for monitoring. The monitoring quantity mainly includes the voltage and current in the front and back stage circuits of the grounding wire. The purpose is to observe the influence of the unbalanced current generated in the circuit on the track circuit when the turnout crosses the regional grounding wire, and to monitor and collect the signal. The layout of the probe is shown in Figure 21.

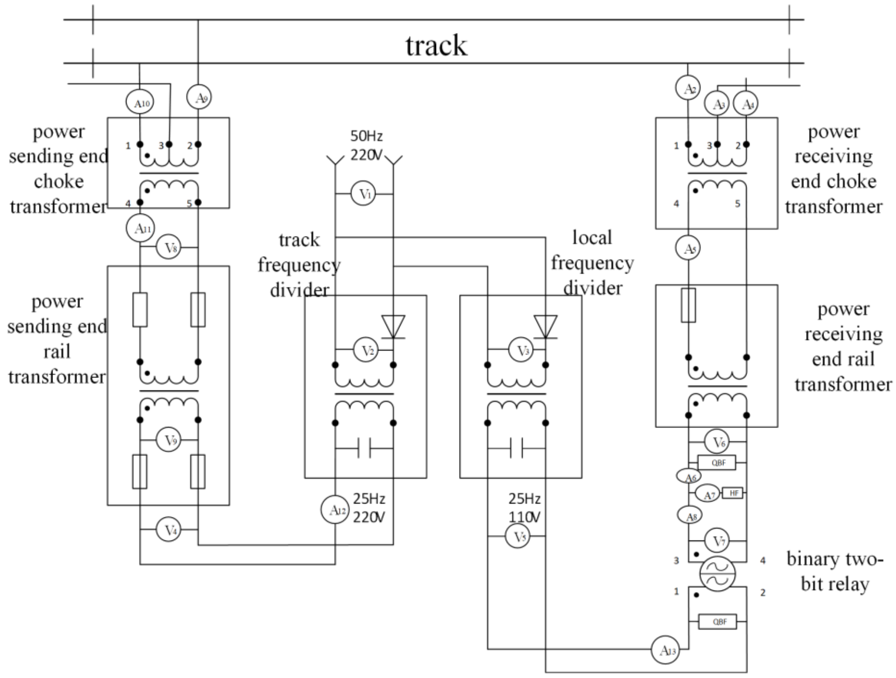

Figure 21. Field probe layout diagram.

Figure 22a shows the voltage and current flowing through the rail when the track circuit is not grounded. At this time, the track circuit is in normal working condition. It can be seen that the unbalanced current flowing in the rail is small, which is 0.8 A. The unbalanced small current is mainly caused by the unbalanced track impedance.

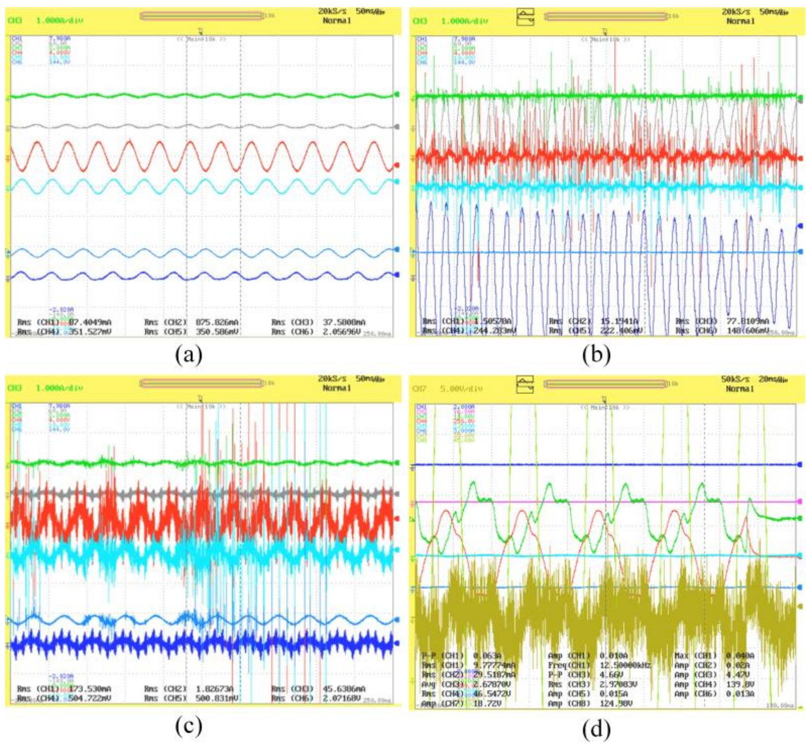

Figure 22. Choke transformer and relay grounding wire test waveform. (**a**) The track circuit is not grounded; (**b**) The position of grounding wire is close to the monitored position; (**c**) The grounding wire is far from the monitored position; (**d**) Waveform distortion during grounding wire hanging.

In order to explore and analyze the influence of the distance between the grounding wire and the monitoring point, the positions near and far from the monitoring point are set up for the grounding wire test. When the position of the grounding wire is close to the monitoring point, it can be found from Figure 22b that the grounding wire has a great influence on the monitoring point, the waveform distortion is serious, and the unbalanced current generated reaches 14 A. When the position of the grounding wire is far away from the monitoring point, the waveform of the choke transformer is shown in Figure 22c. Under the influence of the grounding wire, although there are some waveform glitches, the effective value of the unbalanced current in the track is low, only 1.7 A. Therefore, the grounding wire will lead to the appearance of an unbalanced current, and the value of the unbalanced current is also affected by the distance between the grounding wire and the monitoring point. When the grounding wire is close to the monitoring point, the unbalanced current is larger, and vice versa.

In the process of hanging the grounding wire, the waveform of the track coil side is also disturbed due to the serious distortion of the waveform, as shown in Figure 22d. It can be seen that the voltage waveform of the track coil side drops from the original 22 V voltage to 2.97 V. At this time, the track circuit has produced a red ribbon, and there has been misoperation.

5. Conclusions

In this paper, through the analysis, simulation and field test of the mechanism of misoperation of 25 Hz phase-sensitive track circuit equipment under an unbalanced current, the following conclusions are drawn:

(1) It is explained that the main causes of the track unbalanced current are the unbalanced impedance of the traction current loop, the traction unbalanced current caused by the magnetic field coupling of the adjacent rail traction current and the unbalanced current caused by the grounding wire.

(2) Through the simulation of the excitation current, the flux and core loss of the choke transformer and the flux and core loss of the relay coil under the unbalanced impulse current, the analysis of the influence of the unbalanced current on the choke transformer and the relay are verified. At the same time, it is found that the unbalanced impulse current will lead to the increase of the core loss of the choke transformer and the relay, affecting its life and causing interference to the equipment.

(3) Through the unbalanced current simulation test, an unbalanced current test during driving and the grounding wire test, it is further verified that the magnetic saturation of the choke transformer under unbalanced current interference affects the relay coil voltage, resulting in misoperation. It is found that the unbalanced impulse current will be generated during driving, resulting in the decrease of receiving voltage. At the same time, it is found that the unbalanced current is also affected by the distance between the grounding wire and the measuring point. When the grounding wire is close to the measuring point, the unbalanced current is larger, and vice versa.

Author Contributions: Methodology, B.Z.; Software, M.Z.; Formal analysis, Z.L.; Resources, C.X.; Writing—original draft, L.W.; Writing—review & editing, J.L.; Funding acquisition, J.C. All authors have read and agreed to the published version of the manuscript.

Funding: This research was funded by the research and application of the influence of the electrified railway traction power supply system on the track circuit under grant E19L00700.

Data Availability Statement: The data presented in this study are available in 'Research on Interference Mechanism of 25 Hz Phase Sensitive Track Equipment from Unbalanced Current'.

Conflicts of Interest: The authors declare no conflict of interest.

References

1. Peng, W.; Liu, Q.; Liang, L.; Jiang, W.; Zhang, Z. Design Requirement and DC Bias Analysis on HVDC Converter Transformer. *E3S Web Conf.* **2021**, *257*, 01038. [CrossRef]
2. Junshuang, Z.; Haiming, L.; Wanyi, T.; Lianguang, L.; Mingyang, L. Experiments and simulation analysis of 500kV single-phase three-column transformer in No-load under DC bias. *J. Phys. Conf. Ser.* **2020**, *1585*, 012014. [CrossRef]
3. Xiaobin, C.; Manxiang, W.; Chuanlin, Z.; Yufeng, H. Traction Return Current Distribution and Influencing Factors under Direct Power Supply Mode of Heavy Haul Railway. *China Railw. Sci.* **2021**, *42*, 137–144.
4. Kunpeng, L.; Wei, L.; Qunzhan, L.; Bin, D. Theoretical Analysis of Rail Potential in DC Traction Return System. *Urban Rapid Rail Transit* **2015**, *28*, 91–94.
5. Razghonov, S.; Kuznetsov, V.; Zvonarova, O.; Chernikov, D. Track circuits adjusting calculation method under current influence traction interference and electromagnetic compatibility. *IOP Conf. Ser. Mater. Sci. Eng.* **2020**, *985*, 012017. [CrossRef]
6. Xiaosheng, H. Causes and Countermeasures Analysis of Interference of Electrified Track Circuit. *Public Commun. Sci. Technol.* **2010**, *24*, 71+69.
7. Jianhao, M. Interference Analysis and Protection of Traction Return Current to Signal Control System for Electrified Railways. *Railw. Signal. Commun. Eng.* **2017**, *14*, 85–88.
8. Linlin, Y. Research on Traction Return Current of High Speed Railway. *China Sci. Technol. Expo* **2014**, *28*, 327.
9. Laisheng, J. Discussion on Traction Return Way and Influence in High Speed and Heavy Load Section. *Electr. Railw.* **2006**, 165–168. [CrossRef]
10. Hill, R.J.; Carpenter, D.C. Rail Track Distributed Transmission Line Impedance and Admittance: Theoretical Modeling and Experimental Results. *IEEE Trans. Veh. Technol.* **1993**, *42*, 225–241. [CrossRef]
11. Arghavani, H.; Peyravi, M. Unbalanced current-based tariff. *CIRED Open Access Proc. J.* **2017**, *1*, 883–887. [CrossRef]
12. Tao, J.; Zhipeng, C.; Liang, W. On the Effect of the Traction Returning Current on the Track Circuit in the Direct Power Supply System and Our Counter-Measures. *Traffic Eng. Technol. Natl. Def.* **2019**, *17*, 40–43+65.
13. Huh, J.S. Study on voltage unbalance improvement using SFLC in pewer feed network with electric railway system. *IEEE Trancaction Appl. Supercond.* **2005**, *23*, 1219–1228.
14. Youpeng, Z.; Junli, L.; Bin, Z. Research on interference of the unbalanced traction return current to circuit for broken rail detection. *Chin. J. Eng. Des.* **2013**, *20*, 446–452.
15. Isaicheva, A.G.; Basharkin, M.V.; Zolkin, A.L.; Losev, A.N.; Giniyatullina, D.R. Estimation of electrical energy losses in a DC traction rail network during heavy traffic. *IOP Conf. Ser. Earth Environ. Sci.* **2022**, *990*, 012023. [CrossRef]
16. Abdulkareem, A.; Adesanya, A.; Agbetuyi, A.F.; Alayande, A.S. Novel approach to determine unbalanced current circuit on Nigerian 330kV transmission grid for reliability and security enhancement. *Heliyon* **2021**, *7*, e07563. [CrossRef]
17. Boteler, D.H. Modeling Geomagnetic Interference on Railway Signaling Track Circuits. *Space Weather* **2021**, *19*, e2020SW002609. [CrossRef]
18. Haoyue, Z.; Zang, H.; Wang, R. Research on ZPW-2000A Track Circuit State Diagnosis Based on Set Pair Analysis. *IOP Conf. Ser. Earth Environ. Sci.* **2020**, *571*, 012017.
19. Xu, C. Unbalanced current analysis and novel differential protection for HVDC transmission lines based on the distributed parameter model. *Electr. Power Syst. Res.* **2019**, *171*, 105–115.
20. Yang, L. Calculation of Transformer Core Loss under DC Magnetic Bias Based on Dynamic J-A Hysteresis Model. Master's Thesis, Tiangong University, Tianjin, China, 2018.
21. Hao, Z. Research on the Effects of Geomagnetic Storms on Phase Detecting Track Circuit. Master's Thesis, North China Electric Power University, Beijing, China, 2017.
22. Zanwu, H.; Xueye, W.; Ze, L. Extracting the Characteristic Frequency of High Asymmetric Pulse Disturbed by Impulse. *J. China Railw. Soc.* **2012**, *34*, 71–75.